



ACCEPTED MANUSCRIPT

This is an early electronic version of an as-received manuscript that has been accepted for publication in the Journal of the Serbian Chemical Society but has not yet been subjected to the editing process and publishing procedure applied by the JSCS Editorial Office.

Please cite this article as M. Marković, M. Gorgievski, N. Štrbac, V. Grekulović, M. Zdravković, M. Marković, and D. Stanković, *J. Serb. Chem. Soc.* (2025) <https://doi.org/10.2298/JSC241107017M>

This “raw” version of the manuscript is being provided to the authors and readers for their technical service. It must be stressed that the manuscript still has to be subjected to copyediting, typesetting, English grammar and syntax corrections, professional editing and authors’ review of the galley proof before it is published in its final form. Please note that during these publishing processes, many errors may emerge which could affect the final content of the manuscript and all legal disclaimers applied according to the policies of the Journal.



J. Serb. Chem. Soc. **00(0)** 1-21 (2025)
JSCS-13109

Analysis and statistical modeling of copper ions biosorption onto calcined chicken eggshell

MILJAN MARKOVIĆ^{1*}, MILAN GORGIEVSKI¹, NADA ŠTRBAC¹, VESNA GREKULOVIĆ¹, MILICA ZDRAVKOVIĆ¹, MARINA MARKOVIĆ¹, AND DALIBOR STANKOVIĆ²

¹University of Belgrade, Technical Faculty in Bor, Vojske Jugoslavije 12, Bor, Serbia, and

²University of Belgrade, Faculty of Chemistry, Studentski trg 16, Belgrade, Serbia.

(Received 7 November 2024; revised 5 December 2024; accepted 24 January 2025)

Abstract: The study on the possible use of calcined chicken eggshells as a biosorbent for copper ions removal from aqueous solutions, as well as some comparisons between raw and calcined eggshells, are presented in this paper. SEM-EDS and FTIR analysis of the calcined chicken eggshell samples were performed. In addition, the DTA-TGA analysis on raw chicken eggshells was performed. The influence of various process parameters, such as solution pH, stirring rate, biosorbent mass and Cu²⁺ concentration, was investigated. The kinetic analysis using four different empirical kinetic models was performed. The equilibrium analysis was done using the Langmuir, Freundlich and Temkin isotherm models. The process was optimized using the Response Surface Methodology based on the Box-Behnken Design (RSM-BBD). The obtained results are compared to our previous study on raw eggshells as a biosorbent for Cu²⁺ removal, in order to determine the justification for biosorbent modification (i.e. the calcination of raw eggshells).

Keywords: biosorption; calcined chicken eggshell; equilibrium; kinetics; Box-Behnken design.

INTRODUCTION

Water is a crucial resource that occupies an indispensable position in earth's environment. Its main purpose is to support life. Availability of clean drinking water is of vital importance for human welfare. Unfortunately, in many parts of the world, we face the challenge of low quality water sources, which leads to health concerns. The quality of water has a significant effect on the biodiversity in the aquatic ecosystems as well. Lastly, water is an important constituent in numerous industrial processes.¹

* Corresponding author. E-mail: mmarkovic@tfbor.bg.ac.rs
<https://doi.org/10.2298/JSC241107017M>

Heavy metal pollution originating from wastewater generated by industrial activity is a serious global problem. The importance of removing pollutants, including hazardous heavy metals, is increasing with time, as a consequence of growing demands for clean water all around the world.^{2,3}

One of the widespread water contaminants among heavy metals is copper (Cu^{2+}). Main sources of copper wastewater pollution include mining, metal, electroplating, textile and leather industry. The reported copper concentrations in wastewater from different sources range from 2.5 mg dm^{-3} to 10000 mg dm^{-3} . According to the WHO, maximum Cu^{2+} content in drinking water is 2 mg dm^{-3} . Hence, wastewater treatment in order to remove this pollutant is crucial.^{3,4}

Various processes are used for wastewater treatment on an industrial scale, including chemical precipitation, ion exchange, reverse osmosis, ultrafiltration, coagulation and flocculation, etc. However, these processes are not suitable for treating wastewater contaminated with heavy metals in low concentrations. Adsorption is considered a more suitable treatment method for wastewater with low concentrations of heavy metals. Adsorption can be described as a process of mass transfer, which consists of transferring the adsorbate from the solution to the surface of the adsorbent, where it is bound by physical and/or chemical interactions.^{5,6}

The removal of heavy metals from wastewater by inexpensive biosorbents has been the focus of numerous scientific studies in recent years. This process is called biosorption. The biosorption process involves the use of inactive biomass as an adsorbent. Therefore, the mechanism of removal of the pollutants is complex and is usually based on mechanisms such as ion exchange, adsorption, chelation, chemisorption, precipitation, or their combination.^{6,7}

Eggshells are considered waste, which is a product of the food industry that can be a potential biosorbent due to its high calcium content. Eggshell biomass has no utility value, no specific application and in most cases is disposed of as biowaste in landfills. The possible use of eggshells in the biosorption process thus solves several problems. First of all, the use of eggshells as a biosorbent would lead to a reduction in the amount of waste in landfills, thus helping industries which use of eggs by reducing the cost of disposing of their waste. On the other hand, the use of eggshells as a biosorbent for treating wastewater contaminated with heavy metals would help solve the problem of environmental pollution.⁷

The main purpose of this research is the evaluation of the possibility of using a modified form of chicken eggshell (calcined chicken eggshell) as a biosorbent for copper ions removal from aqueous solutions. This work is a continuation of a previous study on the use of raw chicken eggshells for Cu^{2+} removal from aqueous solutions.⁸ Therefore, it analyses the difference in the efficiency in Cu^{2+} removal of the modified eggshell in comparison to the raw eggshell, as well as the other differences between the two processes. This analysis serves as an answer to the

question whether the use of additional resources and energy for the modification of the eggshells is justified. Additionally, the potential use of eggshells (raw or calcined) as a biosorbent could prove to be very important from more than one point of view, as mentioned above. Firstly, the removal of Cu^{2+} ions from wastewaters would have a significant effect on environmental pollution. Secondly, the use of a waste product, such as eggshells, would help solving the landfill problem.

EXPERIMENTAL

Biosorbent

Raw chicken eggshell (RCE) were crushed, sieved through a set of laboratory sieves, and the fraction (-1+0.4) was used for further preparation of the biosorbent. The eggshells were rinsed with distilled water, dried, and then calcined in a laboratory furnace, at 900 °C, for one hour. The obtained calcined chicken eggshell (CCE) sample was used as a biosorbent for the Cu^{2+} biosorption experiments.⁹

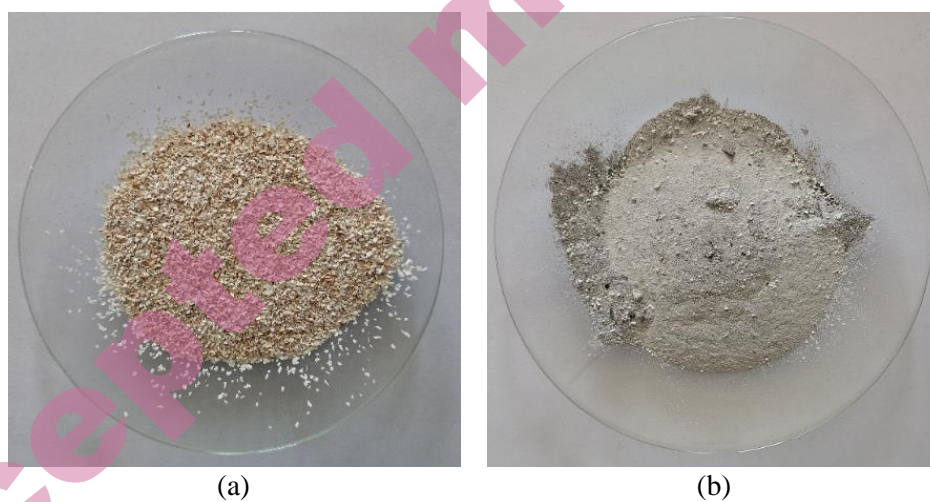


Figure 1. (a) RCE sample, and (b) CCE sample

MATERIALS AND METHODS

The biosorption experiments were performed with synthetic copper ions solutions prepared with $\text{CuSO}_4 \cdot 5\text{H}_2\text{O}$ (p.a. purity). The pH of the solutions was adjusted using 0.1 M KOH, and 0.1 M HNO_3 solutions. The chemicals used were manufactured by LACHEMA (Czech Republic).

The concentration of Cu^{2+} ions in the solutions was determined on a Spectroquant Pharo 300 spectrophotometer (Merck). The pH value of the solution was measured using a pH meter JENCO VisionPlus, while the conductivity of the solution was measured by the WTW inoLab cond - 720 conductometer. The DTA-TGA analysis was performed on a simultaneous DSC-DTA-TGA device SDT Q600 (TA Instruments). FTIR analysis of the samples was performed on a Smart iTR Nicolet iS50 spectrophotometer (Thermo Fisher Scientific, USA). The surface morphology of the samples was recorded using the SEM-EDS method on a VEGA 3 LMU

TESCAN scanning electron microscope with X-act SDD 10 mm² energy-dispersive X-ray analysis (Oxford Instruments).

The biosorption capacity and metal removal degree were calculated using the equations (1) and (2):

$$q_t = \frac{C_i - C_t}{m} V \quad (1)$$

$$\text{RD}\% = \left(1 - \frac{C_t}{C_i}\right) \cdot 100 \quad (2)$$

where: q_t - is the biosorption capacity defined as mass of the adsorbed metal per unit mass of the biosorbent (mg g⁻¹) at time t ; C_i and C_t - are the initial and final concentrations of metal ions (g dm⁻³) at time t ; V - is the volume of the solution used in the biosorption experiments (dm³); and m - is the mass of the biosorbent (g); RD% - is the removal degree (%).

All the experiments, bar the thermodynamic analysis, were performed at room temperature.

Calcined eggshells characterization

The DTA-TGA of the eggshell sample was performed in order to obtain information about the thermal stability and degradation of this material. The eggshell sample was heated in an inert atmosphere from 20 to 900 °C. The SEM-EDS analysis was performed on CCE samples before and after the Cu²⁺ biosorption process. FTIR analysis was performed on CCE samples taken before the biosorption of copper, and after, to determine which functional groups interact with Cu²⁺ in the process of binding these ions to the structure of the adsorbent. The FTIR spectrum of the calcined chicken eggshell samples was recorded in the range from 4000 to 400 cm⁻¹. The sample was placed on a diamond plate and fixed using a pressure tower. Prior to the measurements, a signal of the background was recorded and automatically subtracted by an accompanying OMNICTM software. The copper-loaded CCE was prepared for the characterization analysis by bringing into contact 1 g of the samples with Cu²⁺ solutions (initial concentration 5 g dm⁻³, and the pH value of the solutions 4.5) for 90 minutes.

The influence of different process parameters on biosorption efficiency

A series of experiments were carried out to determine the influence of pH on biosorption capacity. 50 cm³ Cu²⁺ solutions (initial concentration 5 g dm⁻³) with pH values ranging from 2 to 5 were brought into contact with 1 g CCE samples, for 60 minutes, and the biosorption capacity was analyzed. The pH values were adjusted using 0.1 M KOH and 0.1 M HNO₃.

The effect of initial copper ions concentration on the biosorption capacity was analyzed by bringing into contact 1 g of CCE samples with 50 cm³ solutions of different Cu²⁺ concentrations, in the range from 0.5 to 20 g dm⁻³. The pH value of the solutions was 4.5. The suspensions were stirred for 60 minutes, and the biosorption capacity was analyzed.

The influence of the mass of the biosorbent on the biosorption degree was analyzed by bringing into contact 50 cm³ of Cu²⁺ solutions (2 g dm⁻³ initial concentration) with different amounts of CCE samples, ranging from 0.1 to 2 g, and stirring the suspensions for 60 minutes. The pH value of the solutions was 4.5

The effect of stirring rate on the biosorption degree was evaluated by bringing into contact 1 g of CCE with 50 cm³ copper ions solutions (initial Cu²⁺ concentration 5 g dm⁻³, and the pH value of the solutions 4.5) at different stirring rates, ranging from 100 to 600 rpm. The contact between phases was sustained for 60 minutes, after which the suspension was filtered and the filtrate analyzed.

Biosorption kinetic study and determination of activation energy

Kinetic models can be used to analyze the experimental data, to obtain information about the biosorption rate and its mechanism. To obtain the experimental kinetic data, CCE (1 g) were brought into contact with 50 cm³ of Cu²⁺ solutions (initial concentration 5 g dm⁻³, and the pH value of the solutions 4.5) at different contact times, ranging from 1 to 90 minutes. The obtained experimental data were analyzed using four kinetic models: the pseudo-first order kinetic model (Eq. (3)), the pseudo-second order kinetic model (Eq. (4)), the Weber-Morris kinetic model (Eq. (5)), and the Elovich kinetic model (Eq. (6)). These models can be expressed as follows:^{9,10,11}

$$\frac{dq_t}{dt} = k_1(q_e - q_t) \quad (3)$$

$$\frac{dq_t}{dt} = k_2(q_e - q_t)^2 \quad (4)$$

$$q_t = k_i t^{1/2} + C_i \quad (5)$$

$$\frac{dq_t}{dt} = \alpha e^{-\beta q_t} \quad (6)$$

where: q_t - is the biosorbent capacity defined as the mass of the adsorbed metal per unit mass of the biosorbent (mg g⁻¹) at time t ; q_e - is the biosorbent capacity defined as the mass of the adsorbed metal per unit mass of the adsorbent (mg g⁻¹) at equilibrium; and k_1 - is the biosorption rate constant for the pseudo-first order kinetic model (min⁻¹); k_2 - is the biosorption rate constant for the pseudo-second order kinetic model (g mg⁻¹ min⁻¹); k_i - is the internal particle diffusion rate constant (mg g⁻¹ min^{-0.5}); and C_i - is a constant that provides insight into the thickness of the boundary layer; α - is the starting biosorption rate (mg g⁻¹ min⁻¹); β - is the parameter that expresses the degree of surface coverage and activation energy for chemisorption (g mg⁻¹).

Biosorption equilibrium study

The equilibrium study of the biosorption process provides insight into the interaction between metal ions and biosorbents, which helps to determine the effectiveness and the mechanism of the process.¹²

The biosorption isotherm data was obtained by bringing into contact 1 g of CCE samples with 50 cm³ Cu²⁺ solutions of different initial concentrations, in the range from 0.5 to 10 g dm⁻³. The pH value of the solutions was 4.5 The suspension was stirred for 60 minutes, filtered and the filtrate analyzed. The obtained experimental data were fitted with three different isotherm models. The used models were: the Langmuir isotherm model (Eq. (8)), the Freundlich isotherm model (Eq. (9)) and the Temkin isotherm model (Eq. (10)).⁸

$$q_e = \frac{q_m K_L C_e}{1 + K_L C_e} \quad (7)$$

$$q_e = K_f C_e^{1/n} \quad (8)$$

$$q_e = B \ln(K_T C_e) \quad (9)$$

where: C_e - is the equilibrium concentration of metal ions (mg dm⁻³); q_e - is the equilibrium adsorption capacity (mg g⁻¹); q_m - is the maximum adsorption capacity (mg g⁻¹); and K_L - is the Langmuir equilibrium constant (dm³ g⁻¹); K_f - is the Freundlich equilibrium constant ((mg g⁻¹) (dm³ mg⁻¹)^{1/n}); $B = RT/b$ - is the Temkin constant, which refers to the adsorption heat (J mol⁻¹); b - is the variation of adsorption energy (J mol⁻¹); R - is the universal gas constant (J mol⁻¹ K⁻¹); T - is the temperature (K); K_T - is the Temkin equilibrium constant (dm³ g⁻¹).

Biosorption thermodynamic study

The thermodynamic parameters were determined by bringing into contact 1 g of CCE with 50 cm³ of Cu²⁺ solutions (initial concentration 5 g dm⁻³) for 60 minutes, at different temperatures, in the range from 25 °C to 45 °C. The obtained results were used to calculate the thermodynamic parameters using the following equations:⁸

$$K_d = \frac{C_A}{C_S} \quad (10)$$

$$\Delta G^\ominus = -RT \ln K_d \quad (11)$$

$$\ln K_d = \left(\frac{\Delta S^\ominus}{R}\right) - \left(\frac{\Delta H^\ominus}{RT}\right) \quad (12)$$

where: K_d - the thermodynamic equilibrium constant; C_A - the concentration of the adsorbed adsorbate (mg dm⁻³); C_S - the equilibrium concentration of the adsorbate in the solution (mg dm⁻³); ΔG^\ominus - the Gibbs free energy (kJ mol⁻¹); R - the universal gas constant (J mol⁻¹ K⁻¹); T - the temperature (K); ΔS^\ominus - the entropy change (J mol⁻¹ K⁻¹); ΔH^\ominus - the enthalpy change (kJ mol⁻¹).

Biosorption optimization study

Copper ions biosorption using CCE as a biosorbent was optimized using the Box-Behnken experimental design in order to determine the effects of three selected variables on the efficiency of Cu²⁺ removal. The RSM (Response Surface Methodology) is an experimental design used to predict and model relationships between independent and dependent factors and one or more responses.¹³ The Box-Behnken factor experimental design, which consists of 17 experiments, was applied to optimize the biosorption process by analyzing and comparing the three selected factors: adsorbent mass (A), initial copper ion concentration (B) and contact time (C). The test series and their values are listed in Table I.

Table I. Experimental design (experimental ranges and their levels)

Factors	Range level		
	-1	0	1
A – Adsorbent mass, g	0.5	1	1.5
B – Initial metal ion concentration, g dm ⁻³	5	7	10
C – Contact time, min	10	60	90

RESULTS AND DISCUSSION

DTA-TGA analysis of chicken eggshells

Thermal analysis of the chicken eggshells sample was performed in order to determine the changes that occur during the calcination process. The obtained results are shown on Figure 4.

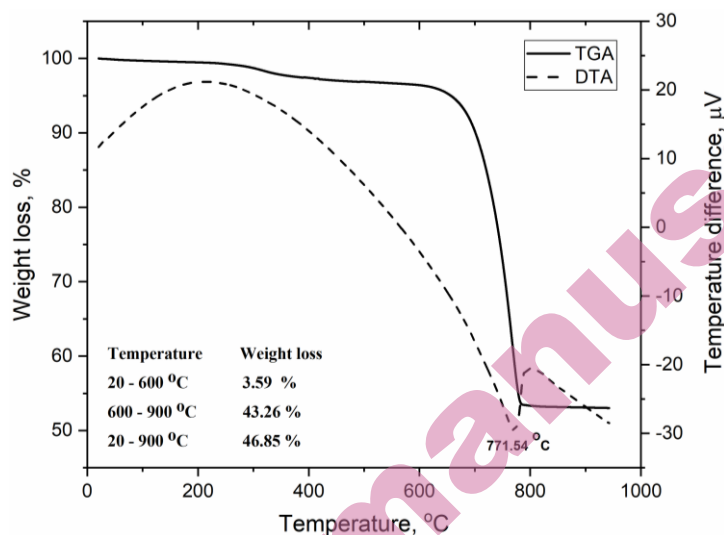


Figure 2. DTA-TGA analysis of the RCE sample

The TGA curve, given on Figure 2, shows two stages of weight loss of the sample during the heating/calcination process. In the range from 20 to 600 °C, a weight loss of 3.59 % was recorded, corresponding to the decomposition of organic matter (proteins), as well as the release of the structurally bound water (moisture). In the range from 600 to 900 °C, a weight loss of 43.26 % was observed, which can be attributed to the decomposition of calcium carbonate, during which CO₂ gas is released. This process is accompanied by an endothermic peak on the DTA curve, with a maximum at 771.54 °C. This stage marks the transformation of the chicken eggshell sample into stable CaO. The total weight loss was 46.85 %. Similar findings were reported in the work of Witoon T.¹⁴

SEM-EDS analysis of CCE before and after the Cu²⁺ biosorption

The results of the SEM analysis of the CCE sample before and after the Cu²⁺ biosorption are shown on Figure 3. The obtained EDS analysis is given in Table II.

The morphology of the RCE sample, was examined in the previous work. The obtained results given in the previously published work suggested that the surface morphology of the RCE sample was mainly porous.⁸ A change in the surface morphology of the eggshell samples can be noted after calcination (Figures 3(a) and (b)), as the calcination process led to the forming of an irregular structure, consisting of agglomerates and flakes of different sizes (from 1 up to 500 μm).^{15,16} The SEM image of the CCE sample after the biosorption is given on Figures 3(c) and (d). It can be noted that the particles were partially agglomerated after the interaction between the Cu²⁺ solution and the biosorbent. The irregular structure is

still present, but the particles are somewhat larger in size, with the present flakes partially agglomerated.

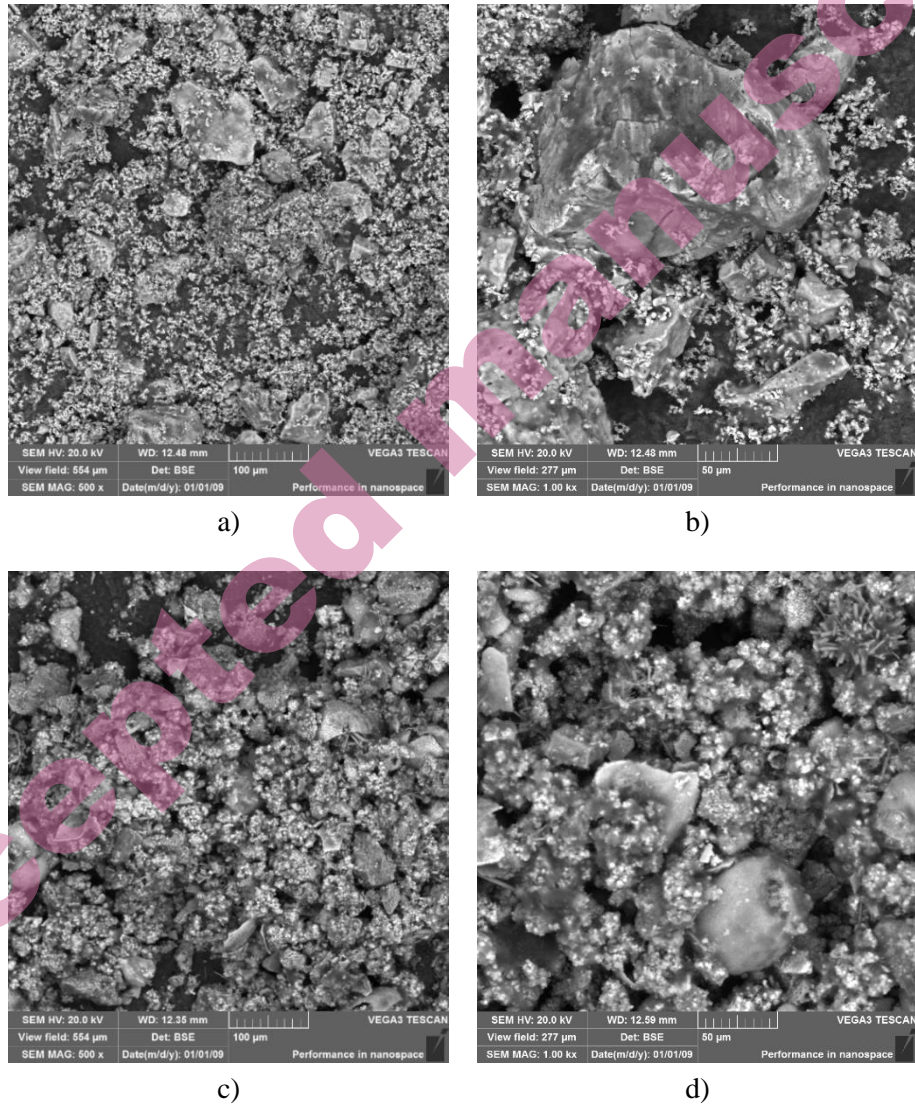


Figure 3. SEM micrograph of the CCE before at 500x (a) and 1000x (b) and after the biosorption process at 500x (c) and 1000x (d)

Table II. The EDS analysis of the CCE samples before and after the biosorption process

Before Cu ²⁺ biosorption	Element	O	Mg	K	Ca	Cu	Total
	Content, mas. %	58,7	0,67	0,53	40,1	/	100
After Cu ²⁺ biosorption	Element	O	Mg	K	Ca	Cu	Total
	Content, mas. %	49,19	/	/	14,89	35,92	100

The EDS analysis of the CCE samples before the biosorption process shows that Ca, Mg, and K are present. The EDS analysis after Cu²⁺ biosorption showed a significant decrease in the Ca content, while the Mg and K disappeared completely, as well as an appearance of Cu on the surface of the analyzed sample. The changes showed by the EDS analysis indicate that Ca, Mg and K could potentially be involved in the biosorption process. The RCE EDS analysis obtained in the previous research showed similar results.⁸

FTIR analysis of the raw RCE sample and CCE sample before and after Cu²⁺ biosorption

The results of the FTIR analysis of the raw RCE and CCE sample before and after Cu²⁺ biosorption are shown on Figure 4.

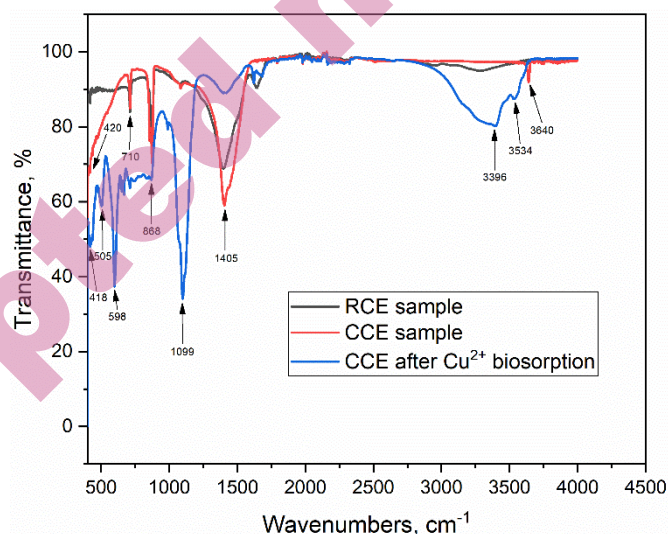


Figure 4. FTIR spectra of the raw RCE sample, as well as CCE samples before and after copper ions biosorption

The tested samples showed the correct behavior expected for this type of analyte, with all characteristic peaks present. The peaks appearing at the low-end of the spectrum of the CCE sample, below 500 cm⁻¹ as well as the peak at 710 cm⁻¹, can be attributed to the Ca-O bond, which indicates to the conversion of CaCO₃ to CaO. The obtained FTIR spectra of the raw RCE sample and the CCE sample before the biosorption process shows peaks at around 710 and 869 cm⁻¹ indicate to the out-plane and in-plane deformation of C=O, respectively. These peaks, and the

peak observed at 1405 cm^{-1} can be strongly associated with the presence of CaCO_3 in the samples.^{17,18,19} These results indicate that the decarbonization and transformation of CaCO_3 to CaO did occur during the calcination process, but it was not complete, as the presence of both the calcium oxide and carbonate was confirmed by the FTIR analysis of the CCE sample.

A sharp peak is observed at 3640 cm^{-1} before the biosorption process, which is contributed to the O-H stretching vibration and the bending hydroxyl groups, which indicate to the presence of Ca(OH)_2 . The Ca(OH)_2 was formed as CaO adsorbed water.^{20,21}

The spectra recorded after the Cu^{2+} biosorption shows bands at 418 and 505 cm^{-1} , that can be attributed to the metal-oxygen bonds. The peaks between 650 and 868 cm^{-1} correspond to the hydrogen bonding frequencies originating from the bending vibrations of Cu-O-H. The band recorded at 1100 cm^{-1} , which appears after the biosorption process, is attributed to the sulfate group, originating from $\text{CuSO}_4 \cdot 5\text{H}_2\text{O}$ used for the preparation of the solutions. The broad peaks recorded between 3300 and 3500 are connected to the stretching of the O-H originating from molecular water.^{21,22}

The influence of different process parameters on biosorption efficiency

The influence of pH on the biosorption efficiency

The influence of the *pH* value of the solution on the biosorption capacity is shown on Figure 5a. The obtained results indicate that the biosorption capacity increases with the increase in the *pH* of the solution. As the *pH* increased from 2 to 5, the biosorption capacity rose from 148 mg g^{-1} (*pH* = 2) to 225 mg g^{-1} (*pH* = 5). The *pH* value influence is in accordance with the results showed by RCE, however the biosorption capacity by CCE was recorded to be over 10 times higher (10.82 at *pH* 2 and 21.62 at *pH* 5 reported for RCE).⁸ With the *pH* value increase, the concentration of OH^- ions also increases, which leads to an overall negative charge of the biomass. This leads to higher biosorption capacities, as the Cu ions in the solution are positively charged. It is considered that, at higher *pH* values, the precipitation of Cu^{2+} ions in the form of Cu(OH)_2 also occurs. This phenomenon could be another reason for the big difference between the biosorption capacities of CCE and RCE.^{8,23,24}

The effect of the initial Cu^{2+} concentration on the biosorption efficiency

The effect of the initial copper ions concentration on the biosorption capacity is shown on Figure 5b. As can be seen, the biosorption capacity increases with the increase in the initial Cu^{2+} concentration, up to 272 mg g^{-1} at $10\text{ g dm}^{-3}\text{ Cu}^{2+}$. The increase in the biosorption capacity with higher initial metal ions concentration can be attributed to the higher probability of collision between the copper ions and the biosorbent as a larger amount of metal ions are available for biosorption.²⁵

The influence of biosorbent mass on the biosorption efficiency

The analysis of the influence of biosorbent mass on the efficiency of the process is shown on Figure 5c. The obtained results indicate that the biosorption degree rises rapidly with increasing mass of biosorbent. The maximum biosorption degree was obtained at 0.5 g of CCE (98 %). As the Figure 5c shows, the biosorption degree remained constant with further increase in the biosorption mass.

The effect of stirring rate on the biosorption degree

The experimental results shown on Figure 5d show that the biosorption degree rises from 67% to 98% between 100 and 300 rpm. A slight decrease in the biosorption degree was noted between 300 and 400 rpm, after which there is no significant change in the biosorption degree.

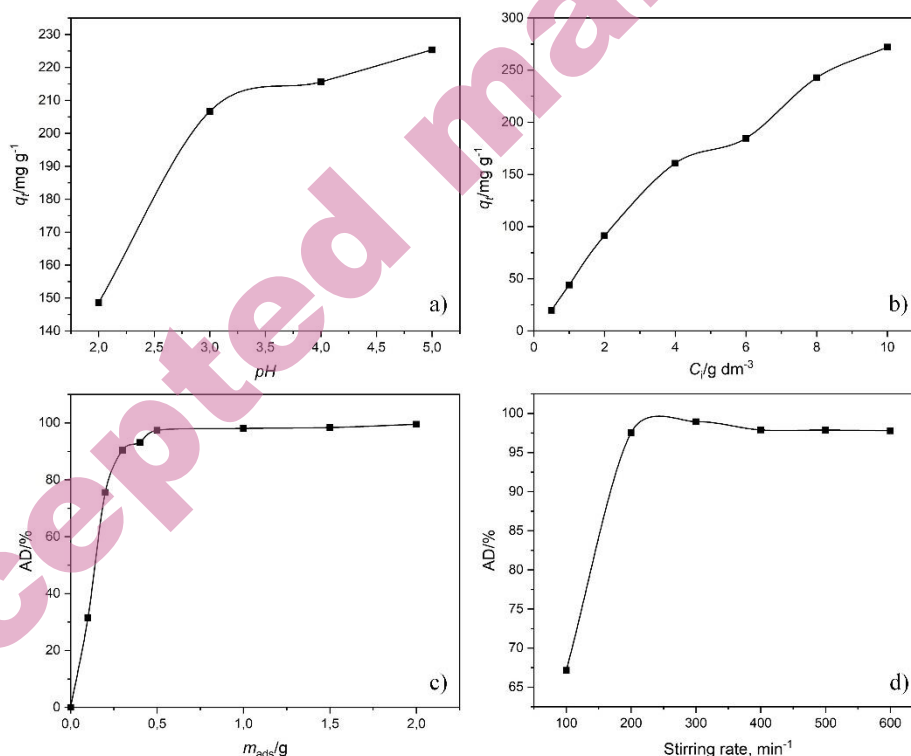


Figure 5. The influence of pH value (a), initial copper ions concentration (b), biosorbent mass (c), and stirring rate (d) on the biosorption efficiency

Biosorption kinetic study

The kinetic analysis of the obtained experimental data, using the pseudo-first order, pseudo-second order, intraparticle diffusion and Elovich kinetic models (Equations 3, 4, 5 and 6) is shown on the Figure 6. The obtained kinetic parameters are given in Table III.

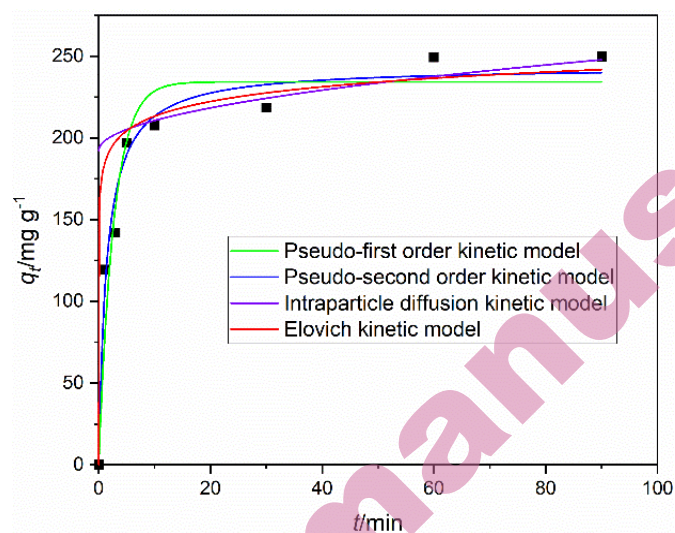


Figure 6. Kinetic data for copper ions biosorption onto CCE

Table III. The values of kinetic parameters for copper ions biosorption onto CCE

Model	Parameters	Values
Pseudo-first order kinetic model	k_1/min^{-1}	0.371
	$q_{e,\text{exp}}/\text{mg g}^{-1}$	234.36
	$q_{e,\text{cal}}/\text{mg g}^{-1}$	249.68
	R^2	0.913
Pseudo-second order kinetic model	$k_2/\text{g mg}^{-1} \text{min}^{-1}$	0.003
	$q_{e,\text{exp}}/\text{mg g}^{-1}$	234.47
	$q_{e,\text{cal}}/\text{mg g}^{-1}$	249.68
	R^2	0.971
Weber-Morris kinetic model	$k_i/\text{g mg}^{-1} \text{min}^{-0.5}$	5.88
	$C_i/\text{mg g}^{-1}$	192.11
	R^2	0.247
	Elovich kinetic model	$\alpha/\text{mg g}^{-1} \text{min}^{-1}$
$\beta/\text{g mg}^{-1}$		0.077
R^2		0.698

The obtained kinetic data, given in Table III, indicates that the pseudo-second order kinetic model is the best fit for the Cu^{2+} ions biosorption onto CCE. This model suggests that the chemical interaction between the CCE samples and the copper ions from the solution was the rate-determining phase of this process, i.e. that chemisorption is the predominant mechanism of binding of copper ions to CCE.¹⁰ Comparing the obtained results to the work on the RCE,⁸ it can be noted that the process of binding copper ions onto CCE is significantly faster, with the experimentally obtained biosorption capacity being 10 times higher than the one recorded in the experimental analysis of Cu^{2+} biosorption onto RCE. The two

processes do not share the same binding mechanisms, as they follow different kinetic models.

Biosorption equilibrium study

The biosorption experimental data were fitted using the Langmuir, Freundlich and Temkin isotherm models (Equations 7, 8 and 9), and the obtained results are shown on Figure 7.

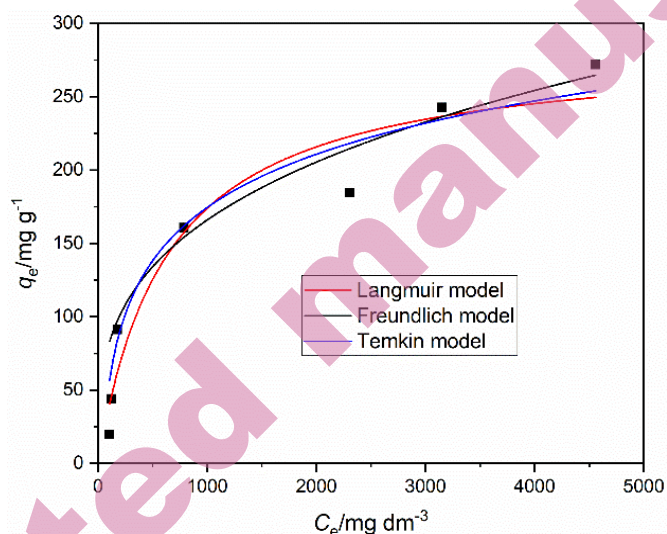


Figure 7. Isotherm data for copper ions biosorption onto CCE

Table IV. Isotherm parameters for copper ions biosorption onto CCE

Model	Parameters	Values
Langmuir isotherm model	$K_L/\text{dm}^3 \text{ mg}^{-1}$	0.002
	$q_{e,\text{exp}}/\text{mg g}^{-1}$	234.36
	$q_m/\text{mg g}^{-1}$	284.12
	R^2	0.941
Freundlich isotherm model	K_F	19.79
	$1/n$	0.308
Temkin isotherm model	R^2	0.944
	$B/J \text{ mol}^{-1}$	52.39
	$K_T/\text{dm}^3 \text{ mg}^{-1}$	0.028
	R^2	0.981

The obtained isotherm parameters (Table IV) indicates that the Temkin isotherm model is the best fit for the experimental data ($R^2 = 0.981$). This model is based on the assumption that the heat of the adsorption of all molecules in the layer decreases linearly with the coverage of the molecules and that the binding energies are uniformly distributed, up to a maximum binding energy.²⁶

The obtained Freundlich constant n indicates that the process of binding Cu^{2+} onto CCE is a favorable process ($1/n$ is lower than 1).²⁷

The maximum biosorption capacity is a parameter which is used to analyze the performance of a biosorbent. The maximum theoretical biosorption capacity for Cu^{2+} ions biosorption onto RCE was 94.59 mg g^{-1} , as reported in the previous work.⁸ In comparison, the maximum biosorption capacity for Cu^{2+} biosorption onto CCE (Table IV) is 284.12 mg g^{-1} . It can be concluded that the calcination of the eggshells leads to a significant increase in its biosorption capacity.

Biosorption thermodynamics

The Gibbs free energy for copper ions biosorption on CCE was calculated using the Eq. (11). The ΔH^\ominus and ΔS^\ominus parameters were determined from the plot $\ln K_d$ vs $1/T$ (Figure 8). The obtained results are given in Table V.

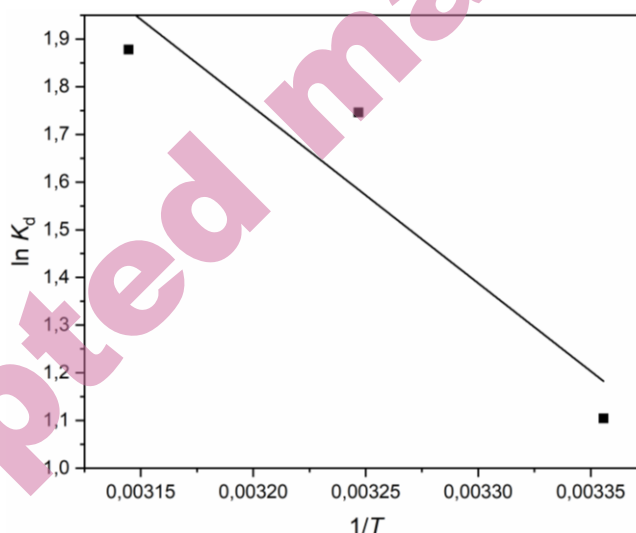


Figure 8. Thermodynamic plot $\ln K_d$ vs $1/T$ for copper ions biosorption onto CCE

Table V. Thermodynamic parameters for copper ions biosorption onto CCE

T/K	$\Delta G^\ominus / \text{kJ mol}^{-1}$	$\Delta H^\ominus / \text{kJ mol}^{-1}$	$\Delta S^\ominus / \text{J mol}^{-1} \text{K}^{-1}$
298	-2.74		
303	-4.47	3.69	13.56
313	-4.96		

The negative ΔG^\ominus values indicate that the process of biosorption of Cu^{2+} ions on CCE is spontaneous and more favorable at higher temperatures.²⁸

Positive ΔH^\ominus and ΔS^\ominus values indicate that this process is endothermic and that increased randomness is present at the contact interface between Cu^{2+} and CCE. The positive enthalpy also confirmed that increasing the system temperature would lead to an increase in the efficiency of copper removal.²⁹

Biosorption optimization study

The process of copper ions biosorption onto CCE was optimized using Response Surface Methodology, with the help of the Box-Behnken Design. The experimental design, given in Table I, was applied to optimize the analyzed process. The resulting test series and their values are listed in Table VI. The matrix of the experimental design and the reaction R (biosorption degree) are shown in Table VI.

Table VI. Box-Behnken Design matrix for three factors along with observed response for Cu²⁺ biosorption onto the CCE

Run	A: Adsorbent mass, g	B: Initial Cu ²⁺ ions concentration, g L ⁻¹	C: Contact time, min	R: Adsorption degree, %
	1	0		98.785
	0	0		98.391
	-1	-1		82.168
	0	0		94.055
	0	-1		31.45
	0	1		72.555
	1	1		77.127
	0	1		11.003
	0	0		97.499
	0	-1		98.482
	1	-1		97.901
	-1	1		38.526
	1	0		24.243
	0	0	0	91.56
	-1	0		50.614
	-1	0		13.818
	0	0	0	98.42

A polynomial equation (14) was fitted in order to describe the correlation between the independent variables: linear ($\beta_1, \beta_2, \beta_3$), quadratic ($\beta_{11}, \beta_{22}, \beta_{33}$), interaction terms ($\beta_{12}, \beta_{13}, \beta_{23}$) and the response (R):³⁰

$$R = \beta_0 + \beta_1 A + \beta_2 B + \beta_3 C + \beta_{11} AA + \beta_{22} BB + \beta_{33} CC + \beta_{12} AB + \beta_{13} AC + \beta_{23} BC \quad (14)$$

The results obtained are shown in Table VI. The copper ions biosorption onto CCE can be expressed as:

$$R = 95.99 + 14.12A - 13.85B + 29.99C + 5.72A \cdot B + 9.44A \cdot C - 1.37B \cdot C - 14.28A^2 - 7.77B^2 - 34.84C^2 \quad (15)$$

The ANOVA analysis was used to assess the statistical significance of the applied model, and the results are given in Table VII. The significance of the individual coefficients is analyzed by the F-values and P-values. The coefficient is more significant as the corresponding F-value is larger and P-value lower. P-values

The obtained F-value of 115.83 means that the model is significant. This further indicates that there is only a 0.01% chance that a F-value of this magnitude can appear due to noise.

P-values of less than 0.0500 provide further proof to the significance of the used model. In this research, A, B, C, AB, AC, A², B², C² are considered significant terms. P-values above 0.1000 indicate that the model terms are not significant.

The 2.86 lack of fit F-value indicates that the lack of fit is not significant. There is a probability of 16.78% that such a large lack of fit F-value can occur due to noise.

The obtained F and P-values of the model (115.83 and 0.0001, respectively) show that the model is significant. P-values below 0.05 indicate that the model terms are significant. The model fit was also confirmed by the regression coefficients of the predicted and experimental values ($R^2 = 0.993$ and $\text{adj-}R^2 = 0.985$).

The diagram of actual versus predicted responses is shown in Figure 9. The obtained results show a very good agreement between the predicted and experimental data.

Figure 10 shows 3D surface plots that illustrate the influence of the selected parameters on the response (R). Figure 10a shows that a lower initial metal ion concentration in combination with a higher adsorbent mass leads to a very high biosorption efficiency (ANOVA analysis indicated to a significant combination of these two factors (A and B)). Figure 10b shows the interaction between the adsorbent mass and the contact, indicating that higher values of these factors lead

to a high percentage of metal removal, and the ANOVA analysis also confirms that the combination of these factors is significant. Figure 10c shows that lower initial metal ion concentrations and longer contact time lead to a high metal removal percentage.

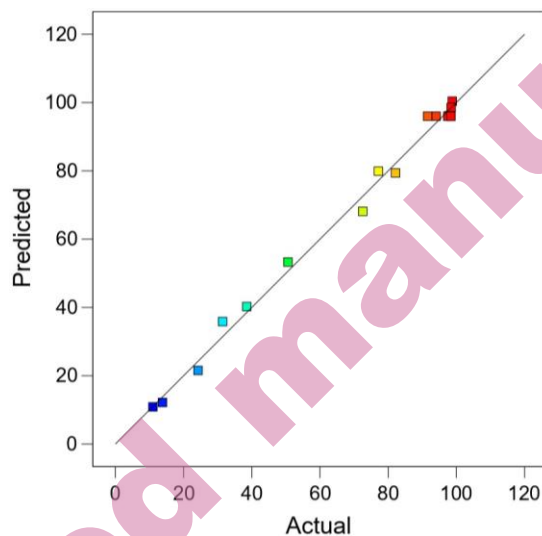


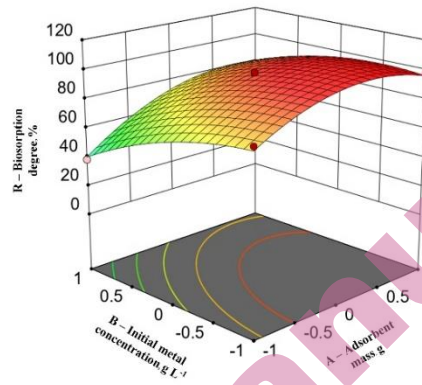
Figure 9. Actual vs predicted responses

The optimization of the biosorption process of copper ions onto CCE was performed using the RSM-BBD method. The influence of the mass of the biosorbent, the initial metal ion concentration and the contact time was evaluated. The model used proved to be statistically significant. The analysis showed that all model terms and most of their interactions were significant. The model suggests that the optimal biosorption conditions are: 90 min contact time, 1 g biosorbent mass and 5 g dm⁻³ initial Cu²⁺ concentration.

Design Points:
 ● Above Surface
 ○ Below Surface
 11.003 98.785

X1 = A
 X2 = B

Actual Factor
 C = 0

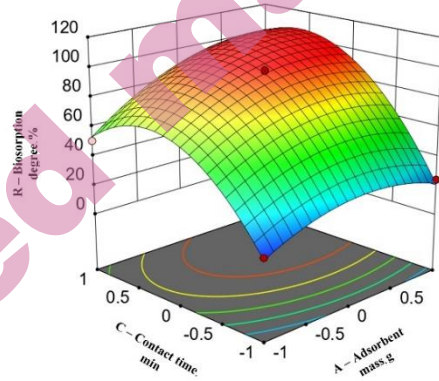


a)

Design Points:
 ● Above Surface
 ○ Below Surface
 11.003 98.785

X1 = A
 X2 = C

Actual Factor
 B = 0

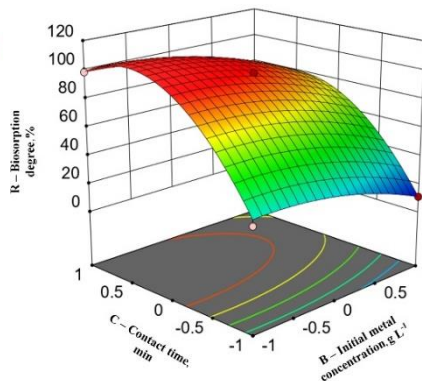


b)

Design Points:
 ● Above Surface
 ○ Below Surface
 11.003 98.785

X1 = B
 X2 = C

Actual Factor
 A = 0



c)

Figure 10. Response surface plots showing the interaction and influence on the biosorption rate (R) of (a) adsorbent mass (A) and initial copper ions concentration (B); (b) adsorbent mass (A) and contact time (C); (c) initial copper ions concentration (B) and contact time (C)

CONCLUSIONS

The DTA-TGA analysis of the eggshells sample indicated to the formation of stable CaO during the calcination process. These findings were confirmed by the FTIR analysis, which showed the presence of both CaO and CaCO₃.

The SEM analysis of the CCE showed that an irregular structure consisting of agglomerates and flakes of different sizes formed during the calcination process.

The kinetic analysis showed that the pseudo-second order kinetic model is the best fit for the analyzed data, indicating that chemisorption is the predominant mechanism for the binding of copper ions onto CCE.

The equilibrium analysis indicated that the Temkin model showed the best agreement with the experimental data. This analysis also indicated that the calcination of the eggshells leads to a significant increase in their maximum biosorption capacity.

The thermodynamic analysis showed that this process is beneficial and endothermic at higher temperatures and that there is an increased randomness at the interface between Cu²⁺ and CCE.

The process of biosorption of copper ions onto CCE was optimized using response surface methodology based on the Box-Behnken design. The influence of biosorbent mass, initial Cu²⁺ ion concentration and contact time on the degree of biosorption was analyzed and modeled. ANOVA analysis showed that the model used and all three parameters analyzed were significant. The optimal parameter values were determined (90 min contact time, 1 g of biosorbent and 5 g dm⁻³ Cu²⁺ concentration).

The maximum experimentally obtained biosorption capacity for the biosorption of copper ions on CCE was 284.12 mg g⁻¹. Comparing this result to the work on RCE⁸, it can be concluded that the modification of the eggshells (calcination) increases their biosorption capacity around 10 times.

ИЗВОД

АНАЛИЗА И СТАТИСТИЧКО МОДЕЛИРАЊЕ БИОСОРПЦИЈЕ ЈОНА БАКРА НА
КАЛЦИНИСАНОЈ ЉУСКОЈ ПИЛЕЊЕГ ЈАЈЕТА

МИЉАН МАРКОВИЋ¹, МИЛАН ГОРГИЈЕВСКИ¹, НАДА ШТРБАЦ¹, ВЕСНА ГРЕКУЛОВИЋ¹, МИЛИЦА ЗДРАВКОВИЋ¹,
МАРИНА МАРКОВИЋ¹, ДАЛИБОР СТАНКОВИЋ²

¹Универзитет у Београду, Технички факултет у Бору, Војске Југославије 12, Бор, Србија, и ²Хемијски факултет, Универзитет у Београду, Сивуђенски тир 12-16, Београд, Србија.

У овом раду представљена је студија о могућој употреби калцинисаних љуски пилећих јаја као биосорбента за уклањање јона бакра из водених раствора, као и поређење између сирових и калцинисаних љуски јаја. Извршене су SEM-EDS и FTIR анализе узорака калцинисаних љуски пилећих јаја. Поред тога, спроведена је DTA-TGA анализа сирових љуски јаја. Испитиван је утицај различитих параметара процеса, као што су рН вредност раствора, брзина мешања, маса биосорбента и концентрација Cu²⁺ јона. Кинетичка анализа

је извршена коришћењем четири различита емпиријска кинетичка модела. Анализа равнотеже је спроведена применом Лангмировог, Фројндлиховог и Темкиновог модела изотерми. Процес је оптимизован коришћењем Методологије површине одзива на основу Vox-Behnken дизајна (RSM-BBD). Добијени резултати су упоређени са претходном студијом о употреби сирових љуски јаја као биосорбента за уклањање Cu^{2+} јона, како би се утврдила оправданост модификације биосорбента (односно калцинације сирових љуски јаја).

(Примљено 7. новембра 2024; ревидирано 5. децембра 2024; прихваћено 24. јануара 2025.)

REFERENCES

1. M. Anandh Babu, S. Hemavathi, G. Kousalyadevi, S.P. Shanmuga Priya, *Glob. NEST J.* **25** (2023) 1 (<https://doi.org/10.30955/gnj.005287>)
2. A. H. Jendia, S. Hamzah, A. A. Abuhabib, N. M. El-Ashgar, *Water Supply* **20** (2020) 2514 (<https://doi.org/10.2166/ws.2020.151>)
3. R. Ratnawati, A. Prasetyaningrum, H. Hargono, M. F. Zakaria, *Period. Polytech. Chem. Eng.* **68** (2024) 239 (<https://doi.org/10.3311/PPch.22867>)
4. Y. Liu, H. Wang, Y. Cui, N. Chen, *Int. J. Environ. Res. Public Health* **20** (2023) 3885. (<https://doi.org/10.3390/ijerph20053885>)
5. P. Musonge, C. Harripersadth, *Mater. Res. Forum* **91** (2021) 171 (<https://doi.org/10.21741/9781644901144-5>)
6. S. A. Al-Saydeh, M. H. El-Naas, S. J. Zaidi, *J. Ind. Eng. Chem.* **56** (2017) 35 (<https://doi.org/10.1016/j.jiec.2017.07.026>)
7. K. Vijayaraghavan, U. M. Joshi, *Environ. Eng. Sci.* **5** (2017) 180532 (<https://doi.org/10.1098/rsos.180532>)
8. M. Marković, M. Gorgievski, N. Štrbac, V. Grekulović, K. Božinović, M. Zdravković, M. Vuković, *Metals* **13** (2023) 206 (<https://doi.org/10.3390/met13020206>)
9. R. Slimani, I. E. Ouahabi, F. Abidi, M. El Haddad, A. Regti, M. R. Laamari, S. El Antri, S. Lazar, *J. Taiwan Inst. Chem. Eng.* **45** (2013) 1578 (<https://doi.org/10.1016/j.jtice.2013.10.009>)
10. M. Samimi, *Glob. J. Environ. Sci. Manag.* **10** (2023) (<https://doi.org/10.22034/gjesm.2024.01.03>)
11. H. Qiu, B. Pan, Q-j. Zhang, W. Zhang, Q-x. Zhang, *J. Zhejiang Univ. – Sci. A* **10** (2009) 716 (<https://doi.org/10.1631/jzus.A0820524>)
12. K. M. Elsherif, R. A. Abdullah Saad, A. M. Ewlad-Ahmed, A. A. Treban, A. M. Iqneebir, *Adv. J. Chem. A* **6** (2023) 334 (<https://doi.org/10.48309/ajca.2024.415865.1415>)
13. S. Akazdam, M. Chafi, W. Yassine, L. Sebbahi, B. Gourich, N. Barka, *J. Mater. Environ. Sci* **8** (2017) 784 (https://www.jmaterenvironsci.com/Document/vol8/vol8_N3/82-JMES-ICMES-Akazdam.pdf)
14. T. Witoon, *Ceram. Int.* **37** (2011) 3291-3298 (<https://doi.org/10.1016/j.ceramint.2011.05.125>)
15. T. E. Kose, B. Kivanc, *Chem. Eng. J.* **178** (2011) 34 (<https://doi.org/10.1016/j.cej.2011.09.129>)

16. O. G. Agbabiaka, I. O. Oladele, A. D. Akinwekomi, A. A. Adediran, A. O. Balogun, O. G. Olanakanm, T. M. A. Olayanju, *Sci. Afr.* **8** (2020) e00452 (<https://doi.org/10.1016/j.sciaf.2020.e00452>)
17. Y. Erdal, M.N.M. Al-Nuaimy, M. Saleh, Z. Isik, N. Dizge, D. Balakrishnan, *Environ. Res.* **212A** (2022) 113210 (<https://doi.org/10.1016/j.envres.2022.113210>)
18. V. L. Gurav, R. A. Samant, *Orient. J. Chem.* **37** (2021) 128-135 (<http://dx.doi.org/10.13005/ojc/370117>)
19. A. V. Borhade, A. S. Kale, *Appl. Water Sci.* **7** (2017) 4255-4268 (<https://doi.org/10.1007/s13201-017-0558-9>)
20. B. Haddad, A. Mittal, J. Mittal, A. Paolone, D. Villemin, M. Debdab, G. Mimanne, A. Habibi, Z. Hamidi, M. Boumediene, E. Belarbi, *CDC* **33** (2021) 100717 (<https://doi.org/10.1016/j.cdc.2021.100717>)
21. Y. Han, J. Trakulmututa, T. Amornsakchai, S. Boonyuen, N. Prigyai, S. M. Smith, *ACS Omega* **8** (2023) 46663-46675 (<https://doi.org/10.1021/acsomega.3c05758>)
22. M. Kantcheva, *Appl. Catal. B: Environ.* **42** (2003) 89-109. ([https://doi.org/10.1016/S0926-3373\(02\)00218-7](https://doi.org/10.1016/S0926-3373(02)00218-7))
23. L. H. Gai, S. G. Wang, W. X. Gong, X. W. Liu, B. Y. Gao, H. Y. Zhang, *J. Chem. Technol. Biotechnol.* **83** (2008) 806 (<https://doi.org/10.1002/jctb.1869>)
24. M. Yunus Pamukoglu, F. Kargi, *Process Biochem.* **41** (2006) 1047-1054 (<https://doi.org/10.1016/j.procbio.2005.11.010>)
25. G. C. Domnez, Z. Aksu, A. Ozturk, T. Kutsal, *Process Biochem.* **34** (1999) 885 ([https://doi.org/10.1016/S0032-9592\(99\)00005-9](https://doi.org/10.1016/S0032-9592(99)00005-9))
26. S. Tonk, C. Majdik, R. Szep, M. Suci, E. Rapo, B. Nagy, A.G. Niculae, *Rev. Chim.* **68** (2017) 1951 (<https://doi.org/10.37358/RC.17.9.5800>)
27. P. D. Sasha, S. Chowdhury, M. Mondal, K. Sinha, *Sep. Sci. Technol.* **47** (2012) (<https://doi.org/10.1080/01496395.2011.610397>)
28. M. A. Fawzy, H. M. Al-Yasi, T. M. Galal, R. Z. Hamza, T. G. Abdelkader, E. F. Ali, S. H. A. Hassan, *Sci. Rep.* **12** (2022) 8583 (<https://doi.org/10.1038/s41598-022-12233-1>)
29. M. A. Fawzy, *Adv. Powder Technol.* **31** (2020) 3724 (<https://doi.org/10.1016/j.apt.2020.07.014>)
30. A. Choinska-Pulit, J. Sobolczyk-Bednarek, W. Laba, *Ecotoxicol. Environ. Saf.* **149** (2018) 275 (<https://doi.org/10.1016/j.ecoenv.2017.12.008>).